

Compact dual-band RF rectifier for wireless energy harvesting using CRLH technique

Marwa Jasim Alhily, Nasr Al-Khafaji, Salim Wadi

Communications Department, Engineering Technical Collage-Najaf, Al-Furat Al-Awsat Technical University, Najaf, Iraq

Article Info

Article history:

Received May 4, 2021

Revised Jul 30, 2021

Accepted Aug 4, 2021

Keywords:

CRLH matching network

Dual-band rectifier

RF energy harvesting

ABSTRACT

In this paper, a new dual-band radio frequency (RF) rectifier was designed. The proposed design is a low-profile structure with dimensions of $5 \times 5.5 \text{ mm}^2$ owing to the use of lumped elements rather than the conventional transmission lines which occupy large footprints. This property can be potentially exploited to use the proposed rectifier in high dense rectenna arrays to generate high output direct current (DC) voltages. Furthermore, the proposed design adopts the composite right/left-handed composite right left-handed (CRLH) technique to realize the dual-band structure at frequencies of 1.8 and 2.4 GHz. Afterward, the matching circuit was optimized to make sure that it offers good matching. The frequency response shows good matching at both bands which are about -22 and -25 dB respectively. Eventually, the simulated circuit has a conversion efficiency of 52% and output voltages of 0.5 V at -5 dBm for the two bands.

This is an open access article under the [CC BY-SA](https://creativecommons.org/licenses/by-sa/4.0/) license.



Corresponding Author:

Marwa Jasim Alhily

Communications Department, Engineering Technical Collage-Najaf

Al-Furat Al-Awsat Technical University, Najaf, Iraq

Email: marwah@atu.edu.iq

1. INTRODUCTION

Energy harvesting is a promising technology since the environment of the internet of things (IoT) network depends highly on sensors, which in turn, they need continuous power sources. This is by itself is a big challenge because batteries should be replaced from one time to another, resulting in a task that is a heavy burden. Thus, looking for an alternative source that constantly provides the required power becomes in high demand. One of the solutions is to scavenge the radio frequency radio frequency (RF) power which is always available in space [1]. Also, there are other types of energy sources which are thermal energy [2], solar energy [3], and vibrations energy [4], and each type has advantages over others. The RF power density in space is 0.2 nW/cm^2 - $1 \mu\text{W/cm}^2$ [5]. This power is very low if it is compared to other sources. However, this does not prevent researchers from using the RF because of its continuous availability as mentioned before [6]. The RF power is categorized as indoor (e.g., Wifi) and outdoor (e.g., broadcasting, global system for mobile communication (GSM) and digital television (TV)) [7].

A lot of research has been done in this field of power transmission and energy harvesting, but it is rare to see a rectifier design working simultaneously at more than one frequency band with a small footprint [8]. Both these difficulties will be addressed in this paper to come up with a very compact design, capable to harvest the RF power at 1.8 and 2.4 GHz (i.e., a dual-band structure). As a consequence, the proposed design will be potentially a good candidate to work within an array of rectennas to harvest more power from the atmosphere as much as we can.

Various research on single-band matching networks is reported. In [9], a full-wave bridge rectifier is adopted in their design. It is matched only at one single frequency band which is 2.45 GHz and the power is

about 15 dBm. The conversion efficiency obtained from the rectifier was about 61% at the same frequency. The design is suitable for power more than 10 dBm owing to four diodes. For power less than 0 dBm, it is preferred to use a single diode to reduce turn-on power consumption. Furthermore, the circuit is bulky in size and costly. Chandravanshi and Akhtar [10] also working to realize high output direct current (DC) voltage. Thus, they have used a two-stage Dickson charge pump configuration. As in [9], it has high losses due to a large number of used components. Another work designed at 2.45 GHz and input power 10dBm is reported in [11]. The achieved efficiency was almost 70%. All works, in [9]-[11], have attained conversion efficiencies of more than 60% at high levels of input powers. However, high power is not available for ambient RF energy because it has low power levels and spreads over a wide range of frequencies. To compensate for this deficit, picking up energies from multiple bands in one design was another direction of research and had attracted attention. This aids to collect more power from space.

A dual-band matching network is used in [12], where the amount of scavenged power is raised. The proposed design can work at any arbitrary two frequency bands, where the T-type microstrip matching network is adopted. The conversion efficiency obtained was 50% and 20.1% at frequencies of 2.45 GHz and 5.85 GHz, respectively, at a low input power of -10 dBm and a footprint size of (32.8×24) mm². The one problem which was raised here is a relatively big size design. In [13], a rectifier has two branches and each branch consists of an open radial stub for matching purposes with a size of (60×80×1.6) mm³ which is a very large size as well. Song *et al.* [14], have designed a rectifier, capable of harvesting six bands simultaneously. It has three branches and each branch is matched to operate at two different frequencies. The design was bulky and complicated. In [15] the lowest conversion efficiency attained in this structure was 50% and 40% at frequencies 1.9 and 2.45 GHz respectively at an input RF power of 0 dB. Although the lumped elements were employed in the matching circuit design, the proposed design in [15] has a large footprint of 19×21 mm². We can deduce here that, most works mentioned above, have big footprints and the high-frequency band has lower conversion efficiency compared with a lower band because of the priority of matching to low frequencies. This paper will address these two problems (i.e., size and mismatch at higher frequency). In this paper, the proposed rectifier has a compact size of (5×5.5) mm² relying on the composite right left-handed (CRLH) technique to design a dual-band matching network to obtain a compact size structure compared to [12]-[15], with RF-to-DC conversion efficiencies of more than 50% for the two bands.

The paper is organized as section 2. discusses the theoretical part, design methodology, and procedure. The best topology of a rectifier and diode selection is investigated to fit our design requirements. Then, theoretical calculations of lumped elements to achieve a dual-band CRLH matching circuit are introduced. The proposed matching network can be adjusted to work at any two arbitrary frequencies. In section 3. results and discussion is presented. Finally, section 4 concludes the current research in this paper.

2. GENERAL FORM OF THE CONVENTIONAL ENERGY HARVESTING SYSTEM AND THE PROPOSED DESIGN

The rectifier is an important part of the energy harvesting systems due to its ability to convert RF input signals into DC signals, and then save them in the power storage (i.e., capacitors). If the rectifier performs well, more power can be added to the power storage at the same level as the input power [16]. As a consequence, a good rectifier design requires careful attention with low power consumption and high sensitivity to input power. A block diagram of the conventional rectenna (rectifier and antenna) is shown in Figure 1(a). The receiving antenna captures RF energy from the ambient environment and converts it to alternating current (AC) electrical signal. Typically, antennas have 50-ohm input impedances. Thus, matching circuits become necessary, inserted between the antenna with 50-ohm input impedances and the rectifier because most rectifiers have complex impedances, varying with power and frequency. Matching circuits ensure the maximum transfer of power. Moreover, the matching circuits act to reject any high harmonic, propagated back from the conversion procedure that occurred in diodes into the antenna. The third part which is the rectifier topology (i.e., either a single diode or a combination of diodes) is the core of the rectifier that converts AC to DC power. A complex impedance of the rectifier due to the non-linearity behavior of the diode makes it sensitive to change in frequency, input power, and load. DC, RF, and all higher harmonics are injected into the low pass filter (LPF), which in turn, attenuates all components except the DC one. The load placed at the end-stage represents an equivalent impedance for any real application that will be supplied by power from the rectifier. All these parts operate as one system, but they should be optimized to reach the optimal design [17]. In this work, we have made a noticeable modification on the matching part in the conventional rectifier, see Figure 1(b). A dual-band matching network is utilized. Making a circuit operating at any two arbitrary frequencies is not a simple task. The reason behind that, the rectifier has two different complex input impedances, so that rectifier input impedance is a function with frequency. Moreover, powers and loads can influence the rectifier input impedance.

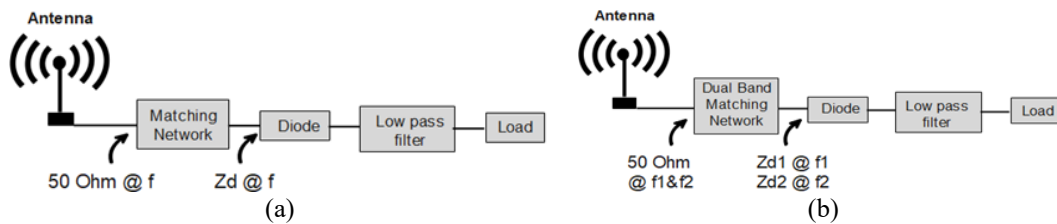


Figure 1. Block diagram of rectenna: (a) conventional rectenna with single-band matching network and (b) proposed rectenna with dual-band matching network

2.1. Rectifier topology

There are a bunch of rectifier typologies and each topology has its benefits over others relying on application and the power density available in space. The most common typologies are the single series diode for low power applications [18] and the voltage doubler for moderate and high power applications [19]. Her single series diode is utilize owing to operate at a low power range of (-5 dBm). A large-signal s-parameter (LSSP) and harmonic balanced (HB) tools in ADS software are used to analyze and compare the rectifier's efficiency. Diodes employed in the analysis are HSMS2850 schottky diodes. This diode type has low forward bias voltage 0.15 v characteristics and fast switching. A vendor model from the ADS library is used with a low pass filter of the series inductor $L=14$ nH and shunt capacitor $C=47$ pF used to eliminate the high order harmonics and to smooth the output voltages.

2.2. CRLH dual-band matching network

Impedance matching network is a key part of most microwave and RF circuits because it ensures the maximum power transfer among parts of the one circuit. Furthermore, it rejects the harmonics propagating backward from one part to another because it acts as a bandpass filter BPF, but with unequal port impedance, unlike the conventional filters. When the microwave circuit operates at a fixed frequency, input power, and fixed load, this leads to the circuit, operating under fixed circumstances. However, as we mentioned earlier, in rectifiers, impedance is variable. Unless the matching circuit is designed carefully, the overall performance will deteriorate with any slight change in the diode impedance. Typically, the matching circuits are designed to operate at only one frequency and this is normal in the RF circuits because they work at that frequency. On the contrary, it is desirable to harvest the ambient power from a wide range of frequencies to collect power as much as we can. As the number of frequency bands is increased, the circuit complexity increases. Both circuit parts and sizes are matter. If lumped elements are used, sizes will be smaller than circuits consisting of transmission circuits, but extra losses introduced by lumped elements will be added. Mostly, the compromise has been made to achieve in between goals. Herein, the goal is to build very small footprint circuits with lumped elements to use in our future works with dense-rectenna arrays. Also, the circuit will be designed at two arbitrary frequencies using the CRLH technique. The CRLH matching network concept was inspired from the metamaterial (MTM) technique that became a very important owing to its usfull carectristic and properties. To implies media with MTM charectirestic, a CRLH unit cell of lumped element was designed from LH for a low frequency and, and relative humidity (RH) for high frequency band. When a low frequency passes the RH capacitor and inductor became open and short, respectively. When high frequency pass LH capacitor and inductor became short and open, respectively. The mathematical analysis of the adopted CRLH technique to design the proposed dual-band matching circuit is introduced in the following discussion. To calculate the complex input impedance of any two-port network, the transmission ABCD parameters are used as (1).

$$Z_{in} = \frac{AZ_L + B}{D + CZ_L} \quad (1)$$

Where Z_L is the load impedance where it consists of real and imaginary parts as in $Z_L = R_L + jX_L$. Values of A, B, C, and D rely on the type of circuit utilized in the matching network and values of lumped elements. This equation is employed to design a dual-band matching network. Besides, it is used to calculate the scattering S-parameters. Various types can be found in [20] regarding dual-band matching networks using lumped elements, but only one type is adopted here to achieve the research task. This circuit is the series-shunt type.

In this paper, the proposed circuit operates at 1.8 and 2.4 GHz. These two frequencies are chosen since they are always available in the space indoor and outdoor. To demonstrate how dual-band matching occurs, let us follow this procedure. First, the circuit is designed at the lower frequency, where the shunt inductance L_L and series capacitance C_R lumped elements are responsible for doing. Then, the series

inductance L_R and shunt capacitance C_R are optimized to match the circuit at the higher frequency of 2.4 GHz. The subscript L stands for the left or lower frequency band, while the subscript R stands for the right or high-frequency band. Due to a rule of thumb, that when selecting a matching component, the component should have more impact in the target band and less effect in the other band. For example, the series inductance L_R is one of the components used to match the circuit at the second frequency, and it should have a zero or close to zero impedance at the first frequency. In other words, this lumped element does not have any impact on matching the other frequency [21]. The ABCD matrix of series-shunt connection can be obtained as [22].

$$\begin{bmatrix} 1 - X_m X_n & jX_m \\ jX_n & 1 \end{bmatrix} \tag{2}$$

Where $jX_m = Z$ and $jX_n = Y$. To compute, the input impedance of series-shunt connection, (1) and (2) can use as (3).

$$Z_{in} = \frac{R_L + j(X_L - X_L^2 X_n - R_L^2 X_n + (1 - 2X_L X_n + R_L^2 X_n^2 + X_L^2 X_n^2) X_m)}{(1 - X_L X_n)^2 + (R_L X_n)^2} \tag{3}$$

In (3) consists of both real and imaginary parts. Hence, the real part, which is R_{in} , is rearranged to obtain X_n as following,

$$X_n = \frac{(R_{in} X_L \pm \sqrt{R_{in} R_L (R_L^2 + X_L^2 - R_{in} R_L)})}{R_{in} (R_L^2 + X_L^2)} \tag{4}$$

X_n should always be real, and to satisfy this situation the expression $R_L - R_{in} + X_L^2/R_L > 0$. After obtaining the X_n term, the X_m term can be calculated by rearranging the imaginary part of the input impedance which is given as (5). In (5), only the term X_m is unknown.

$$X_m = \frac{(R_L^2 + X_L^2) X_n - X_L + \frac{X_{in} R_L}{R_{in}}}{(R_L^2 + X_L^2) X_n^2 - 2X_L X_n + 1} \tag{5}$$

The one deficit of this approach is that the radicands of X_n and X_m must be always a positive value. To overcome this problem, a combination between series-shunt and shunt-series circuit types is used as in [20]. The adopted modification aids to increase the degree of design freedom and ensures that the radicands of X_n and X_m can be either positive or negative values. One of these combinations is the CRLH, is widely used in the last two decades to synthesize dual-band transmission lines. The synthesized transmission lines can be implemented using only lumped elements. The new transmission lines offer compact footprints. However, extra losses added by lumped elements represent the main source of losses, so making a CRLH transmission line, being a combination of lumped elements and conventional transmission lines, is preferred over other combinations. Here in this research, a CRLH transmission line with only lumped elements will be used as mentioned earlier because the proposed energy harvester will be used in a rectenna array in our future work, seeking ones with very small footprints. Figure 2, shows a dual-band CRLH transmission line, acting as a dual-band matching network, connected to a load impedance Z_L varying with the frequency. As known, the CRLH has dual-band pass characteristics, where the resonance coming from the series resonant tank is called series resonance ω_{ES} , and the resonance coming from the shunt resonant tank is called the shunt resonance ω_{SH} . The series and shunt resonant tanks have impedance Z and admittance Y , respectively, given as (6).

$$Z = jX_m = j \left(\omega L_R - \frac{1}{\omega C_L} \right), Y = jX_n = j \left(\omega C_R - \frac{1}{\omega L_L} \right) \tag{6}$$

Where ω is the design angular frequency. X_m and X_n can calculate from (4) and (5) of series shunt connection. Then the component value of C_R, C_L, L_R, L_L can obtain as:

$$C_L = \frac{k^2 - 1}{\omega k (X_{m2} - k X_{m1})} \tag{7}$$

$$L_R = \frac{1}{\omega} \left(X_{m1} + \frac{1}{\omega C_L} \right) \tag{8}$$

$$L_L = \frac{k^2 - 1}{\omega k (X_{n2} - k X_{n1})} \tag{9}$$

$$C_R = \frac{1}{w} \left(X_{n1} + \frac{1}{wL_L} \right) \quad (10)$$

Where K is frequency ratio, $K = f_2/f_1 = W_2/W$ and $K > 1$. f_1 and f_2 are a first and second frequency respectively.

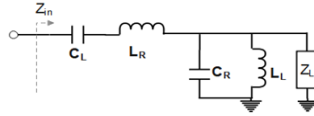


Figure 2. CRLH connection of dual band impedance transforming topology

Having discussed and analyzed all the important information regarding the rectifier and the proposed dual-band impedance transformer, in this work, we will design the proposed dual-band energy rectifier, operating at frequencies 1.8 and 2.4 GHz, but any two arbitrary frequencies can be considered. To evaluate its performance, the reflection coefficient, output voltage, and efficiency are optimized to obtain the best results as much as possible. The input power, load, and frequency are the most three parameters that effectively impact rectifier performance. Thus, trading-off among them is imperative. In all simulations, real-world lumped components from Murata are utilized to make the results closer to the practical ones because each element in Murata has its associated parasitic effects. The circuit schematic is depicted in Figure 3. R_L and C_1 represent the load and the low pass filter, respectively. The larger the R_L is, the larger the output voltage, but is the smaller the efficiency. C_1 can be considered the main storage of the DC power, and it can also work to shorten out the AC signals. The latter function can be carried out with a help of the series inductor L_1 . This inductor tends to have a bigger impedance as the frequency increases, so fundamental and higher harmonics are attenuated to some acceptable extent. In the schematic, D_1 is the diode which is the main component, responsible for the rectification process, while all other remaining elements L_L , C_L , L_R , and C_R form the dual-band matching circuit. Furthermore, the traces connecting among all the circuit components are electromagnetically simulated and then are exported into the main schematic to take into account their losses. This procedure is called co-simulation and is achieved by the ADS software. The final real circuit with the true footprint layout for each lumped element is shown in Figure 4. The Roger Duroid 3010 laminate is used with a relative permittivity of 10.2 and a thickness of 0.5 mm.

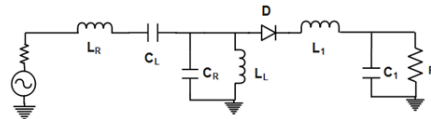


Figure 3. Schematic of rectifier with CRLH dual band matching network transformin. $R_L=1.5$ kohm, $C_1=47$ pF, $L_1=14$ nH, $L_L=4.6$ nH, $C_R=0.2$ pF, $C_L=0.4$ nH, $L_R=6.9$ nH

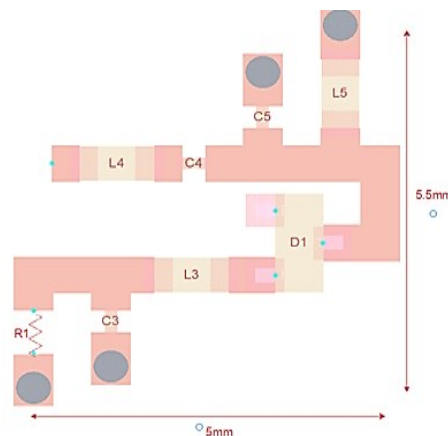


Figure 4. Final topology of the proposed dual-band rectifier where the final size on the PCB is 5×5.5 mm² taken from the ADS software

3. RESULTS AND DISCUSSION (RECTIFIER PERFORMANCE)

The simulated reflection coefficient S11 of the rectifier circuit with different input power levels is depicted in Figure 5(a) with a fixed load resistance of 1.5 kohm. As can be seen, the proposed rectifier is matched very well at frequencies of 1.8 and 2.4 GHz even with varying input power. For both bands, the matching frequency tends to slightly shift to a lower frequency. This means that the matching operates well with the new resonant frequencies. However, the matching of all bands is still satisfactory. Moreover, the frequency range between the two bands has S11 about -6 dB when the input power is equal to -5 dBm, and this could result in a wide-band rectifier which is very useful to harvest more power from space. The rectifier has good matching at -5 dBm where this value is close to the power available from typical sources such as WiFi, cellular and digital TV broadcasting. In Figure 5(b), the input power is fixed at -5 dBm, and the load resistance varies from 1 kohm to 4.5 kohm. Load resistance of 1.5 kohm provides the best results of matching at frequencies of 1.8 and 2.4 GHz because the circuit is optimized at this value. As the input power increases the matching is improved, but the response begins to deteriorate after -5 dBm. This occurs because the diode utilized in the proposed design is dedicated to operating at low power levels.

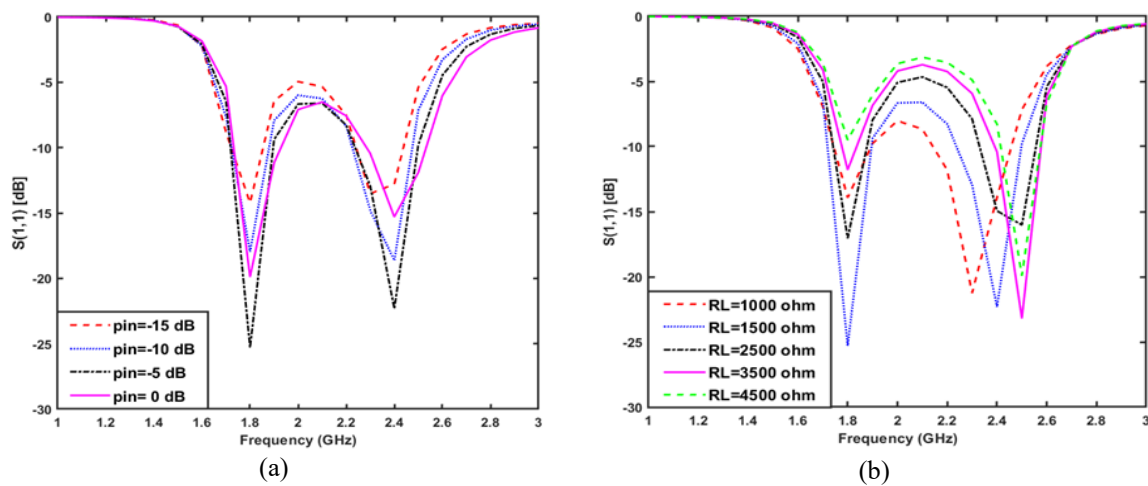


Figure 5. Reflection coefficient S11 of the rectifier with (a) different input power levels and fixed load resistance value of 1.5 kohm and (b) different load resistance values and fixed input power of -5 dBm

The conversion efficiency and the output voltage can be calculated using the formulas given as, [23].

$$Efficiency = \frac{P_{Dc}}{P_{in}} \times 100 \tag{11}$$

and output voltage,

$$V_o = \sqrt{P_{Dc} \times R_L} \tag{12}$$

Here, V_0 and P_{Dc} represent the DC output voltage and DC output power, respectively. P_{in} denotes the input power from the RF source. They are depicted in Figures 6 and 7. When R_L is equal to 1.5 kohm, it gives rise to the highest efficiency, approximately about 53% for both bands, thanks to the benefit of the CRLH dual-band matching network. As the matching increases, more power will be transferred into the load. In other words, the efficiency increases, where the best matching occurs at a load value of 1.5 kohm. Apart from optimum load value, especially when it increases, the efficiency is noticeably decreased. This is reasonable as we stated before. On the contrary, the DC output voltage increases, as the load resistance increases. Even if the output voltage increases, the output DC power decreases, leading to the decrement in efficiency, see Figure 6 for more details. Figure 7 shows the output DC voltage versus frequency for different input power. Also, it increases when increasing the input power, and the output voltage reaches about 0.95 v at frequencies of 1.8 and 2.4 GHz. This voltage decreases to almost half when the input power becomes -5 dBm. The dip between the two bands tends to diminish with decreasing in the input power and the two bands are emerged to be as a single wideband.

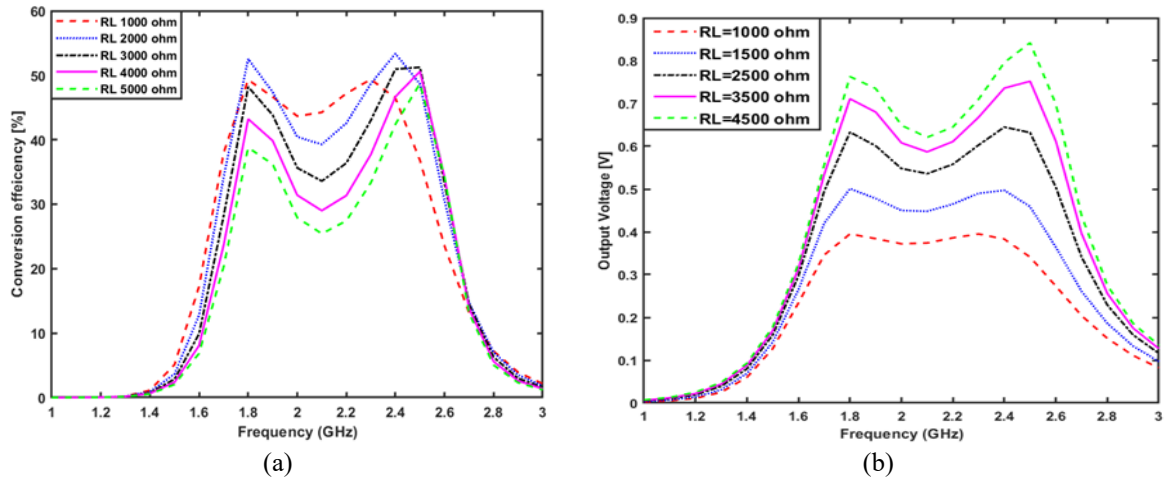


Figure 6. (a) Conversion efficiency vs. frequency for different loads and fixed input power of -5 dBm and (b) output DC voltage vs. frequency for different loads and fixed input power of -5 dBm

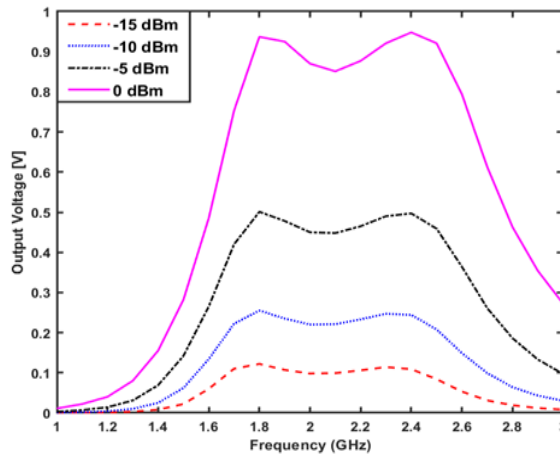


Figure 7. Output DC voltage vs. frequency for different input power and a fixed load of 1.5 kohm

The S11 versus the input power is depicted in Figure 8(a) for 1.8 and 2.4 GHz frequencies. The proposed circuit is well matched at about -5dBm for both bands with large bandwidths. The simulated S11 is less than -20 dB which means that 99% of the input power is transferred into the load if we ignore the losses in lumped elements and transmission lines. Practically, some power will be absorbed and converted into heat. Furthermore, the conversion efficiency at both bands versus the input power is illustrated in Figure 8(b). As can be seen, the efficiencies are almost equal at 0 dBm. After that, the diode fails to convert the power since the input voltage is larger than the diode’s breakdown voltage. The efficiencies are almost 53%. At very low input power. Table 1 compares our present work and others found in the literature. Our proposed design offers the smallest footprint as compared to others according to the best of the authors’ knowledge. It also offers good efficiency if compared to others on the table.

Table 1. Comparison of the proposed rectifier with related work

Frequency (GHz)	Input Power (dBm)	Maximum Conversion Efficiency	Rectifier Size (mm)	Reference
0.915, 2.45	0	37%, 30%	19×21	[17] [2013]
1.8, 2.4	-5	45%	45×8	[24] [2018]
0.925, 2.45	-2.5	65%	15.3×13.7	[25] [2020]
1.8, 2.4	-5	52%	5.5×5	This Work

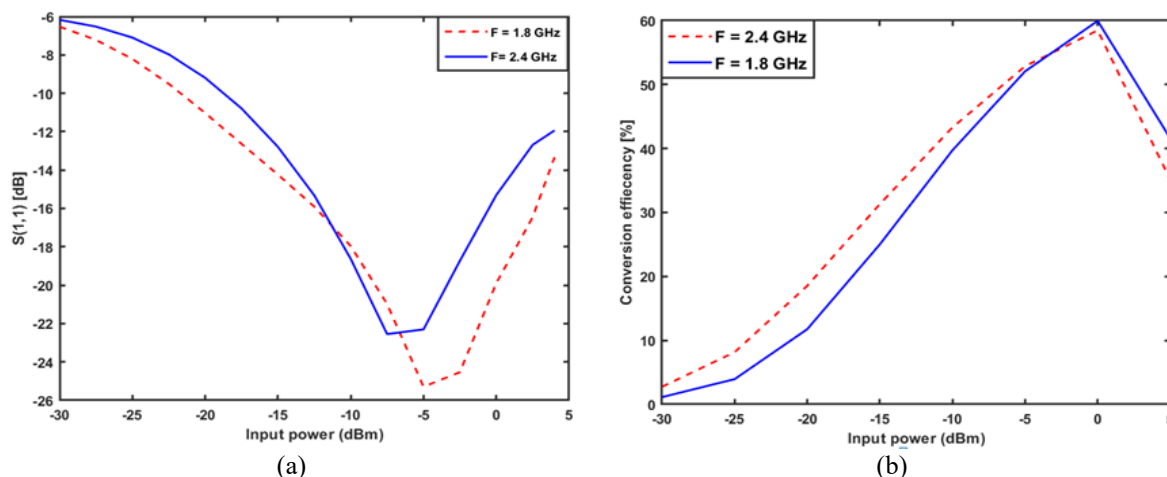


Figure 8. (a) Simulation of S_{11} and (b) Simulation of conversion efficiency. concerning input power at the two frequency band 1.8 and 2.4 GHz and a resistive load of 1.5 kohm

4. CONCLUSION

In this work, a compact dual-band rectifier for a low input power range from -30 to -5 dBm with the single series diode topology using HSMS2850 Schottky diode is implemented, operating at frequencies of 1.8 and 2.4GHz. The composite right/left-handed (CRLH) transmission line technique is used to design the dual-band matching network using only lumped elements. The closed-equations formulas based on dual-band matching network design are derived in this paper, with full explanation, to provide values of the lumped elements. The efficiencies obtained at both prescribed frequency bands are almost the same, being 52%. Moreover, more than 0.5v appears at the load when the input power is -5dBm. The reflection coefficient is -22 and -25 dBm for 1.8 and 2.4 GHz, respectively. The overall size of the rectifier is very small $5.5 \times 5 \text{ mm}^2$ when compared to other related works.

REFERENCES

- [1] R. A. Moffatt, "Wireless power transfer by means of electromagnetic radiation within an enclosed space," *arXiv preprint*, 2016.
- [2] N. Kumari and M. Rokotondrabe, "Thermal network modelling of hybrid piezo-pyro transducer for application in energy harvesting," in *2019 IEEE 5th International Conference for Convergence in Technology (I2CT)*. IEEE, pp. 2019, 1-4, doi: 10.1109/I2CT45611.2019.9033897.
- [3] S. M. Antony, S. Indu, and R. Pandey, "An efficient solar energy harvesting system for wireless sensor network nodes," *Journal of Information and Optimization Sciences*, vol. 41, no. 1, pp. 39-50, 2020, doi: 10.1109/ICPEICES.2018.8897434.
- [4] S. Balgavhar and S. Bhalla, "Green energy harvesting using piezoelectric materials from bridge vibrations," in *2018 2nd International Conference on Green Energy and Applications (ICGEA)*. IEEE, 2018, pp. 134-137, doi: 10.1109/ICGEA.2018.8356282.
- [5] W. Zahra and T. Djeraff, "Ambient rf energy harvesting for dual-band frequencies below 6 ghz," in *2018 IEEE Wireless Power Transfer Conference (WPTC)*. IEEE, 2018, pp. 1-2, doi: 10.1109/ICGEA.2018.8356282.
- [6] B. Munir and V. Dyo, "On the impact of mobility on battery-less rfenergy harvesting system performance," *Sensors*, vol. 18, no. 11, p. 3597, 2018, doi: 10.3390/s18113597.
- [7] M. S. Diagarajan, A. Ramasamy, N. Boopalan, M. Din, and M. Sangaran, "RF energy harvesting prototype operating on multiple frequency bands with advanced power management," *Indonesian Journal of Electrical Engineering and Computer Science (IJECS)*, vol. 17, no. 1, pp. 70-77, 2019, doi: 10.11591/ijeecs.v17.i1.pp70-77.
- [8] U. Muncuk, K. Alemdar, J. D. Sarode, and K. R. Chowdhury, "Multi- band ambient rf energy harvesting circuit design for enabling batteryless sensors and IoT," *IEEE Internet of Things Journal*, vol. 5, no. 4, pp. 2700-2714, 2018, doi: 10.1109/JIOT.2018.2813162.
- [9] F. Erkmen, T. S. Almonneef and O. M. Ramahi, "Scalable electromagnetic energy harvesting using frequency-selective surfaces," *IEEE Transactions on Microwave Theory and Techniques*, vol. 66, no. 5, pp. 2433-2441, 2018, doi: 10.1109/TMTT.2018.2804956.
- [10] S. Chandravanshi and M. J. Akhtar, "Design of efficient rectifier circuit in the GSM band for energy harvesting applications," in *2017 IEEE MTT-S International Microwave and RF Conference (IMaRC)*. IEEE, 2017, pp. 1-5, doi: 10.1109/IMaRC.2017.8449722.

- [11] E. Tammam Sedeek and E. S. Hasaneen, "High efficiency 2.45 ghz low power hybrid junction rectifier for rf energy harvesting," in *2018 International Japan-Africa Conference on Electronics, Communications and Computations (JAC-ECC)*. IEEE, 2018, pp. 147-150, doi: 10.1109/JEC-ECC.2018.8679546.
- [12] M. Ur Rehman, W. Ahmad, and W. T. Khan, "Highly efficient dual band 2.45/5.85 ghz rectifier for rf energy harvesting applications in ism band," in *2017 IEEE Asia Pacific Microwave Conference (APMC)*. IEEE, 2017, pp. 150-153, doi: 10.1109/JEC-ECC.2018.8679546.
- [13] S. Chandravanshi and M. J. Akhtar, "A dual band differential rectifying circuit for rf energy harvester," in *2017 IEEE Asia Pacific Microwave Conference (APMC)*. IEEE, 2017, pp. 491-494, doi: 10.1109/APMC.2017.8251488.
- [14] C. Song *et al.*, "A novel six-band dual cp rectenna using improved impedance matching technique for ambient rf energy harvesting," *IEEE Transactions on Antennas and Propagation*, vol. 64, no. 7, pp. 3160-3171, 2016, doi: 10.1109/TAP.2016.2565697.
- [15] K. Niotaki, S. Kim, S. Jeong, A. Collado, A. Georgiadis, and M. M. Tentzeris, "A compact dual-band rectenna using slot-loaded dual band folded dipole antenna," *IEEE Antennas and Wireless Propagation Letters*, vol. 12, pp. 1634-1637, 2013, doi: 10.1109/LAWP.2013.2294200.
- [16] I. Adam and M. N. M. Yasin, "Rectifier for RF energy harvesting using stub matching," *Indonesian Journal of Electrical Engineering and Computer Science (IJECS)*, vol. 13, no. 3, pp. 1007-1013, 2019, doi: 10.11591/ijeecs.v13.i3.pp1007-1013.
- [17] D. Colaiuda, I. Ulisse, and G. Ferri, "Rectifiers design and optimization for a dual-channel rf energy harvester," *Journal of Low Power Electronics and Applications*, vol. 10, no. 2, p. 11, 2020, doi: 10.3390/jlpea10020011.
- [18] A. Taybi, A. Tajmouati, J. Zbitou, A. Errkik, M. Latrach, and L. El Abdellaoui, "A new design of high output voltage rectifier for rectenna system at 2.45 GHz," *Indonesian Journal of Electrical Engineering and Computer Science (IJECS)*, vol. 13, no. 1, pp. 226-234, 2019, doi: 10.11591/ijeecs.v13.i1.pp226-234.
- [19] J. Tissier, M. Koohestani, and M. Latrach, "A comparative study of conventional rectifier topologies for low power rf energy harvesting," in *2019 IEEE Wireless Power Transfer Conference (WPTC)*. IEEE, pp. 569-572, doi: 10.1109/WPTC45513.2019.9055578.
- [20] B. T. Moon and N.-H. Myung, "A dual-band impedance transforming technique with lumped elements for frequency-dependent complex loads," *Progress In Electromagnetics Research*, vol. 136, pp. 123-139, 2013, doi: 10.2528/PIER12111811.
- [21] Z. Zhang, "Antenna design for mobile devices," John Wiley & Sons, 2017.
- [22] D. M. Pozar, "Microwave engineering," John Wiley & Sons, 2011.
- [23] D. Yeager Sample, M. Buettner and J. Smith, "Development of sensing and computing enhanced passive rfid tags using the wireless identification and sensing platform," *Development and Implementation of RFID Technology*, p. 127, 2017, doi: 10.5772/6521.
- [24] H. Mahfoudi, H. Takhedmit, and M. Tellache, "Dual-band dual-polarized stacked rectenna for rf energy harvesting at 1.85 and 2.45 ghz," *12th European Conference on Antennas and Propagation (EuCAP 2018)*, 2018, pp. 4-118, doi: 10.1049/cp.2018.0477.
- [25] H. Vu Ngoc Anh, N. M. Thien, L. H. Trinh, T. Nguyen Vu, and F. Ferreroet, "Compact dual-band rectenna based on dual-mode metal-rimmed antenna," *Electronics*, vol. 9, no. 9, pp. 1532, 2020, doi: 10.3390/electronics9091532.